Metabolic Engineering ▮ (▮▮▮▮) ▮▮▮–▮▮▮

Contents lists available at ScienceDirect

Metabolic Engineering

journal homepage: www.elsevier.com/locate/ymben

Hepatic anaplerotic outflow fluxes are redirected from gluconeogenesis to lactate synthesis in patients with Type 1a glycogen storage disease

John G. Jones [a,*], Paula Garcia [b], Cristina Barosa [a], Teresa C. Delgado [a], Luisa Diogo [b]

[a] NMR Research Unit, Department of Biochemistry and Center for Neurosciences and Cell Biology, Faculty of Sciences and Technology, University of Coimbra, 3001-401 Coimbra, Portugal
[b] Pediatric Hospital of Coimbra, Portugal

ARTICLE INFO

Article history:
Received 12 November 2007
Received in revised form
23 September 2008
Accepted 26 January 2009

Keywords:
^{13}C NMR
Pyruvate recycling
Anaplerosis
Gluconeogenesis
Isotopomer analysis

ABSTRACT

Hepatic glucose production and relative Krebs cycle fluxes (indexed to a citrate synthase flux of 1.0) were evaluated with [U-^{13}C]glycerol tracer in 5 fed healthy controls and 5 Type 1a glycogen storage disease (GSD1a) patients. Plasma glucose, hepatic glucose-6-phosphate (G6P) and glutamine ^{13}C-isotopomers were analyzed by ^{13}C NMR via blood sampling and chemical biopsy. In healthy subjects, 35±14% of plasma glucose originated from hepatic G6P while GSD1a patients had no detectable G6P contribution. Compared to controls, GSD1a patients had an increased fraction of acetyl-CoA from pyruvate (0.5±0.2 vs. 0.3±0.1, $p<0.01$), and increased pyruvate recycling fluxes (14.4±3.8 vs. 8.7±2.8, $p<0.05$). Despite negligible gluconeogenic flux, net anaplerotic outflow was not significantly different from controls (2.2±0.8 vs. 1.3±0.5). The enrichment of lactate with ^{13}C-isotopomers derived from the Krebs cycle suggests that lactate was the main anaplerotic product in GSD1a patients.

1. Introduction

In Type 1a glycogen storage disease (GSD1a), hepatic glucose-6-phosphatase (G6P-ase) is inactive resulting in major changes of systemic glucose metabolism both upstream and downstream of hepatic glucose-6-phosphate (G6P) (Bandsma et al., 2002a, 2002b). The capacity to maintain plasma glucose levels during fasting is impaired because endogenous glucose cannot be synthesized from either glycogen or gluconeogenic precursors since G6P is a common intermediate for both pathways. Normally, when glucose release via the absorption of dietary carbohydrate is insufficient to meet systemic demand, the balance is supplied by the hydrolysis of hepatic G6P to glucose by glucose-6-phosphatase. In GSD1a patients, the lack of G6P-ase activity means that hepatic carbon fluxes that would normally be destined for glucose production are necessarily redirected to other pathways. Although G6P can be disposed as glycogen, the hydrolysis of glycogen to glucose—which is largely dependent on G6P-ase—is also blocked. This results in the characteristic overabundance of hepatic glycogen, which cannot be relieved by fasting glycogenolysis. Under these conditions, the capacity for converting G6P to glycogen on a daily basis is likely very small and can only account for a very minor portion of G6P flux that is normally destined for endogenous glucose production.[1]

Under both fasting and fed conditions, a significant fraction of hepatic G6P and plasma glucose is derived from gluconeogenic carbons originating from the anaplerotic pathways of the Krebs cycle, with pyruvate being the principal precursor. Gluconeogenesis is considered to account for the majority of anaplerotic outflow from the Krebs cycle (Rognstad and Katz, 1977; Magnusson et al., 1991; Katz et al., 1993; Beylot et al., 1995). Gluconeogenic flux is largely sustained by the conversion of pyruvate to phosphoenolpyruvate (PEP) via pyruvate carboxylase (PC) and phosphoenolpyruvate carboxykinase (PEP-ck). Pyruvate may also be oxidized to acetyl-CoA via pyruvate dehydrogenase (PDH) hence substrate competition between PC and PDH can potentially regulate the rate of pyruvate conversion to G6P (Beylot et al., 1995; Large and Beylot, 1999). Another potential regulatory mechanism is the recycling of PEP to pyruvate via pyruvate kinase that completes a futile cycle (pyruvate→oxaloacetate→PEP→pyruvate) (Rognstad and Katz, 1977; Magnusson et al., 1991; Jones et al., 1997; Diraison et al., 1998; She et al., 2003; Jin et al., 2005). Operation of this cycle may attenuate gluconeogenic flux in two

[1] Fasting hepatic glucose production is ~3 mg/kg/min or 5.4 g/h for a 30 kg child (Kien et al., 1995). Gluconeogenesis contributes ~1.5 mg/kg/min or 2.7 g/h. Assuming a liver mass of 800 g and a glycogen concentration of 0.46 M (Roser et al., 1996), the total hepatic glycogen mass is ~66 g, hence 1 h of glucose production is equivalent to about 10% of the total hepatic glycogen mass.

* Corresponding author.
E-mail address: john.jones@netc.pt (J.G. Jones).

1096-7176/$ - see front matter © 2009 Elsevier Inc. All rights reserved.
doi:10.1016/j.ymben.2009.01.003

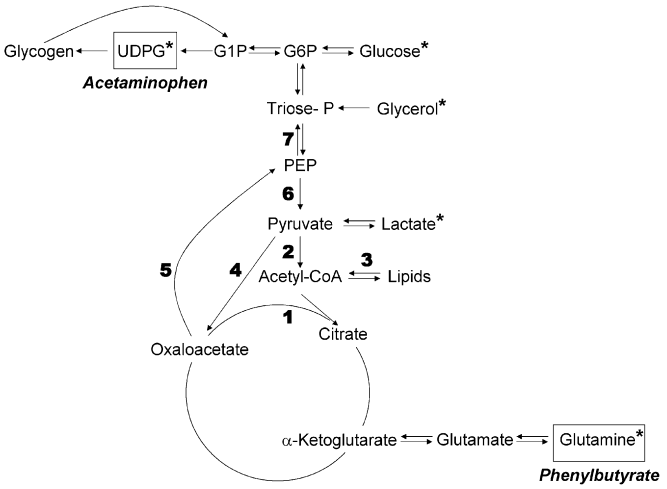

Fig. 1. Hepatic metabolite sampling for ^{13}C-enrichment following the incorporation of ^{13}C from [U-^{13}C]glycerol into hepatic intermediary metabolism in the presence of acetaminophen and phenylbutyric acid. Hepatic UDP-glucose (UDPG) and glutamine are sampled as urinary acetaminophen glucuronide and phenylacetylglutamine (PAGN), respectively. Glucose and lactate are sampled directly from plasma. Also shown are the pyruvate, Krebs cycle and gluconeogenic metabolic pathway components whose relative fluxes are derived from the ^{13}C-isotopomer distribution of PAGN: 1 = citrate synthase flux, 2 = pyruvate dehydrogenase flux, 3 = acyl-CoA oxidation flux, 4 = pyruvate carboxylase flux, 5 = phosphoenolpyruvate carboxykinase flux, 6 = pyruvate kinase flux and 7 = net PEP flux to G6P.

ways: first by redirecting anaplerotic flux from all sources (including anaplerotic substrates that enter the Krebs cycle as 4 and 5-carbon skeletons, such as aspartate, glutamate and glutamine) to pyruvate, and second, by consuming ATP that could otherwise fuel gluconeogenesis. In GSD1a patients, gluconeogenesis is negligible; hence the carbon outflow that would normally be destined for glucose synthesis must either be attenuated by the mechanisms described or redirected into alternative disposal pathways.

To study hepatic G6P-ase and Krebs cycle fluxes, we designed a stable-isotope tracer study that is summarized in Fig. 1. The procedure is non-invasive and can be accommodated into the cornstarch feeding regime of GSD1a patients. [U-^{13}C]Glycerol was used as means of delivering ^{13}C into the hepatic triose-P pool. This substrate has some key advantages in that it is palatable and can be mixed with the cornstarch meal and is also efficiently extracted and metabolized by the liver. [U-^{13}C]Glycerol was accompanied by two xenobiotic agents, acetaminophen and phenylbutyric acid, designed to safely sample key hepatic metabolites as conjugates that are cleared into urine. Acetaminophen is metabolized to acetaminophen glucuronide with the glucuronide moiety derived from UDP-glucose (Hellerstein et al., 1986). Phenylbutyric acid can undergo β-oxidation to phenylacetyl-CoA, which then combines with hepatic glutamine to form phenylacetylglutamine (PAGN) (Comte et al., 2002). Hepatic glutamine is derived in part from the Krebs cycle intermediate α-ketoglutarate, hence the ^{13}C-enrichment distribution of acetyl-CoA and the Krebs cycle can be inferred from PAGN (Yang et al., 1993; Jones et al., 1998, 2001; Diraison et al., 1999). The ^{13}C-enrichment and isotopomer distributions of PAGN and acetaminophen glucuronide, as well as plasma glucose and lactate, can be quantified by ^{13}C NMR following simple extraction and purification procedures (Jones et al., 1998, 2001). The relative activities of anaplerotic and oxidative Krebs cycle fluxes and the pyruvate futile cycle can then be derived from the ^{13}C-enrichment or isotopomer distribution of PAGN (Diraison et al., 1998; Jones et al., 1998, 2001).

2. Methods

2.1. Human studies

Five patients with Type 1a glycogen storage disease (3M, 2F; 14±6 yr; 35±9 kg) and 5 controls (1M, 4F; 20±4 yr; 53±13 kg) were studied following informed consent. For those subjects under 18 years old, informed consent was obtained from the parents. All GSD1a patients were on cornstarch therapy, receiving 1 g/kg of cornstarch every 3 h. The tracer study was incorporated into a set of four cornstarch meals spanning 9 h (Fig. 2). With the second cornstarch meal, subjects ingested 500 mg acetaminophen and with the third meal, subjects ingested 200 mg phenylbutyric acid and 1 g [U-^{13}C]glycerol. Immediately before the final cornstarch meal, 15 ml venous blood was drawn and immediately centrifuged. Plasma was removed and frozen until further processing. Urines were collected over 3-h periods as shown.

2.2. Processing of urinary metabolites and plasma glucose

Urine samples were adjusted to pH 7.0 and incubated overnight with 10,000 U of urease per sample. A trace of sodium azide was also added to inhibit possible infection from airborne microorganisms. The samples were then depleted of protein by addition of perchloric acid, followed by neutralization, centrifugation and lyophilization. Upon reconstitution in 2–3 ml water, the pH was adjusted to 8.0, the sample loaded on to a 16-ml Dowex-1×8-acetate column and washed with 25 ml of water. PAGN and acetaminophen glucuronide were eluted with 35 ml of 10 M acetic acid. This fraction was evaporated and re-suspended in 0.5–1.0 ml water. The pH was adjusted to 7.0 with NaOH, and the samples were centrifuged in Eppendorf tubes. A total of 0.5 ml of the supernatant was introduced into a 5-mm NMR tube and 0.1 ml of deuterated acetonitrile was added to provide a deuterium field-frequency lock signal. Plasma was depleted of protein, neutralized, centrifuged and lyophilized. The lyophilized extract was suspended in 0.6 ml deuterated water and centrifuged, and the supernatant transferred into a 5 mm NMR tube for NMR analysis.

2.3. NMR spectroscopy

Proton-decoupled ^{13}C NMR spectra were acquired at 11.75 T with a Varian Unity 500 system equipped with a 5-mm broadband "switchable" probe with *z*-gradient (Varian, Palo Alto, CA). Spectra were obtained at 50 °C. An acquisition time of 2 s and inter-pulse delay of 1 s were used and the number of acquisitions ranged from 5000 to 25,000. The relative areas of ^{13}C NMR multiplets were quantified using the curve-fitting routine supplied with the NUTS PC-based NMR spectral analysis program (Acorn NMR Inc.,

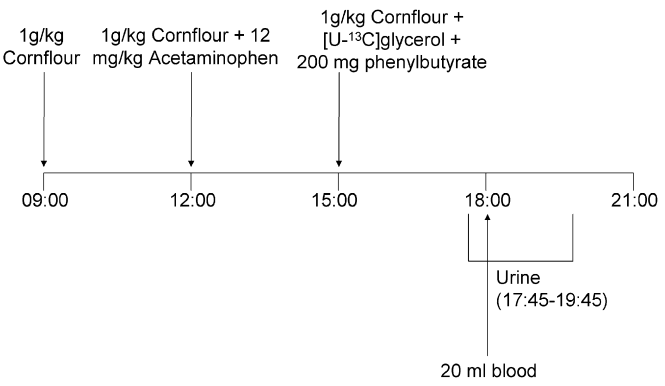

Fig. 2. Tracer and meal administration protocol.

Please cite this article as: Jones, J.G., et al., Hepatic anaplerotic outflow fluxes are redirected from gluconeogenesis to lactate synthesis in patients with Type 1a glycogen storage disease. Metab. Eng. (2009), doi:10.1016/j.ymben.2009.01.003

Fremont, CA). ^{1}H NMR spectra were obtained with the same system and probe with pre-saturation of the water signal.

2.4. Metabolic flux analyses

2.4.1. Main assumptions

The metabolic flux measurements are based on the following general assumptions: (1) isotopic steady-state of the hepatic intermediary metabolite pools (glycolytic/gluconeogenic sugar phosphate intermediates and Krebs cycle metabolites); (2) liver is the principal site of [U-^{13}C]glycerol metabolism (Landau et al., 1996); and (3) oxidative pentose phosphate pathway flux relative to those of gluconeogenesis or glycolysis flux is assumed to be negligible (Magnusson et al., 1988).

2.4.2. Fractional contribution of G6P hydrolysis to plasma glucose

The singlet signal of each resonance was assumed to represent the natural abundance ^{13}C-enrichment of 1.11%. ^{13}C-Excess enrichment in carbons 6 of glucose was estimated from the total area of the ^{13}C–^{13}C spin–spin coupled doublet relative to the central singlet multiplied by 1.11%. Both α and β carbon 6 signals were analyzed. ^{13}C-Excess enrichment in carbon 6 of hepatic G6P was estimated from the glucuronide carbon 6 resonance, which was also resolved into singlet and ^{13}C–^{13}C spin–spin coupled doublet components. Assuming that all glucose excess ^{13}C-enrichment of carbon 6 was derived from carbon 6 of hepatic G6P, the fraction of plasma glucose derived from G6P was estimated as follows:

Excess G6P carbon 6 enrichment (%)
= (glucuronide carbon 6 doublet/carbon 6 singlet)1.11

Excess plasma glucose carbon 6 enrichment
= (plasma glucose carbon 6 doublet/carbon6 singlet)1.11.

Percent of plasma glucose derived from G6P
= 100 × (glucose excess carbon 6 enrichment/G6P excess carbon 6 enrichment).

2.4.3. PAGN ^{13}C-isotopomer analysis and hepatic Krebs cycle fluxes

^{13}C-isotopomers and positional enrichments of the glutamine moiety of PAGN were quantified from the ^{13}C NMR multiplet signals. The singlet signal of each resonance was assumed to represent the natural abundance ^{13}C-enrichment of 1.11%. ^{13}C-Excess enrichment in each of the five glutamine carbons was estimated from the total area of the ^{13}C–^{13}C spin–spin coupled multiplets relative to the central singlet multiplied by 1.11%. Glutamine ^{13}C-isotopomer ratios were quantified from resolved ^{13}C–^{13}C spin–spin coupled multiplet components of each resonance. ^{13}C-Excess enrichment and ^{13}C-isotopomer ratios were applied to tcaCALC (Malloy et al., 1990), a program developed by Dr Mark Jeffrey of the Advanced Imaging Research Center at the University of Texas Southwestern Medical Center at Dallas which is available for download at http://www.utsouthwestern.edu/utsw/home/research/AIRC. There was total of 10 input variables: glutamine carbon 1–4 excess enrichment levels and the following six glutamine ^{13}C-multiplet ratios; carbon 1 doublet/singlet, carbon 2 1,2,3-$^{13}C_3$-quartet/singlet, carbon 2 1,2-$^{13}C_2$-doublet/singlet, carbon 2 2,3-$^{13}C_2$-doublet/singlet, carbon 3 doublet/singlet and carbon 4 doublet/singlet. The ^{13}C NMR isotopomer data were fitted to a standard model of the hepatic Krebs cycle shown in Fig. 1. ^{13}C Input into the Krebs cycle is assumed to be [U-^{13}C]pyruvate derived from the glycolytic metabolism of [U-^{13}C]glycerol. Flux parameters are relative to that of citrate synthase, arbitrarily set to 1.0. The model had 5 degrees of freedom and the uncertainty of each flux parameter was estimated with 100 Monte-Carlo simulations. Fittings were performed systematically starting with a basic Krebs cycle model featuring the simplest set of metabolic conditions (i.e. acetyl-CoA enrichment from labeled pyruvate with no anaplerosis) then adding more parameters until the experimental and calculated ^{13}C-multiplet data showed the best fit (Fonseca et al., 2005). The model accounted for the input of natural abundance ^{13}C as well as enrichment from [U-^{13}C]pyruvate.

3. Results

3.1. Glucose synthesis from hepatic G6P

In the ^{13}C NMR spectrum, ^{13}C-enrichment of glucuronide or glucose from [U-^{13}C]glycerol is resolved from the background natural abundance ^{13}C signal as a result of ^{13}C–^{13}C spin–spin coupling. As illustrated in Fig. 3, the glucuronide carbon 6 resonance has a singlet signal reflecting the natural abundance ^{13}C and a doublet arising from ^{13}C–^{13}C coupling between carbon 6 and the neighboring carbon 5. The doublet signal reflects the excess ^{13}C-enrichment from metabolism of [U-^{13}C]glycerol since its conversion to G6P via [U-^{13}C]triose phosphates results in the formation of multiply-labeled ^{13}C-isotopomers, principally [1,2,3-$^{13}C_3$]and [4,5,6-$^{13}C_3$]G6P. The [4,5,6-$^{13}C_3$]G6P isotopomer contributes to the doublet component of the carbon 6 resonance of glucuronide. The carbon 6α and β resonances of plasma glucose also have doublet components reflecting the conversion of [4,5,6-$^{13}C_3$]G6P to [4,5,6-$^{13}C_3$]glucose. Since ^{13}C-enriched glucose can only be derived from ^{13}C-enriched G6P, the excess enrichments of plasma glucose relative to that of glucuronide directly reflects the fraction of plasma glucose derived from hepatic G6P.

In control subjects, the ^{13}C-signals of both urinary glucuronide and plasma glucose were enriched with ^{13}C indicating hepatic metabolism of [U-^{13}C]glycerol to glucose, as shown in Table 1. In healthy subjects, the fraction of plasma glucose derived from hepatic G6P-ase had a wide inter-individual range 20–50%, possibly reflecting differences in the absorption of unlabeled glucose coupled with variable suppression of hepatic glucose production during the meal. In comparison, GSD1a patients had a significantly reduced level of glucuronide ^{13}C-enrichment and no detectable plasma glucose ^{13}C-enrichment. The absence of excess plasma glucose ^{13}C-enrichment confirms that no plasma glucose was derived from hepatic G6P in any of the five patients. The reduced levels of glucuronide enrichment suggest that flux from G6P to UDP-glucose was lower in these patients compared to healthy controls. The possibility that reduced glucuronide enrichment could reflect reduced uptake and metabolism of [U-^{13}C]glycerol is discounted by the appearance of ^{13}C-enrichment in other sites such as the hepatic Krebs cycle and plasma lactate. Analysis of the carbon 5 glucuronide signal revealed that in addition to the

Please cite this article as: Jones, J.G., et al., Hepatic anaplerotic outflow fluxes are redirected from gluconeogenesis to lactate synthesis in patients with Type 1a glycogen storage disease. Metab. Eng. (2009), doi:10.1016/j.ymben.2009.01.003

expected [4,5,6-$^{13}C_3$]G6P isotopomer, there was also lesser amounts of [5,6-$^{13}C_2$]G6P present (data not shown). The latter isotopomer most probably arises from the metabolism of [U-^{13}C]glycerol to [U-^{13}C]pyruvate, followed by conversion to G6P via gluconeogenesis. As a result of label exchange and randomization at the level of oxaloacetate, the [U-^{13}C]pyruvate moiety is converted to a ~50/50 mixture of [U-^{13}C]PEP and [2,3-$^{13}C_2$]PEP isotopomers. Gluconeogenesis of [2,3-$^{13}C_2$]PEP results in the formation of [5,6-$^{13}C_2$]G6P. The activity of the futile pyruvate cycle increases the amount of [2,3-$^{13}C_2$]PEP at the expense of the [U-^{13}C]PEP isotopomer. The presence of [5,6-$^{13}C_2$]G6P confirms that a portion of the [U-^{13}C]glycerol tracer was metabolized via hepatic Krebs cycle and is consistent with the observation of PAGN ^{13}C-isotopomers (derived from α-ketoglutarate).

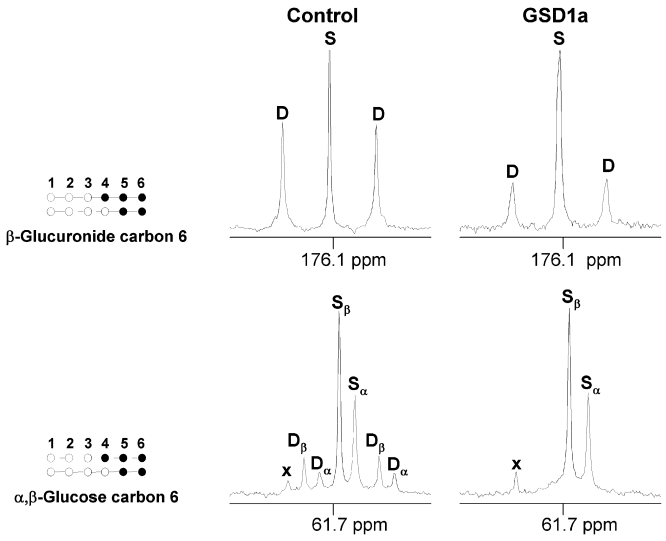

Fig. 3. ^{13}C NMR signals of acetaminophen β-glucuronide carbon 6 and plasma glucose α, β carbon 6 from a healthy control and from a GSD1a patient. Where noted, each NMR signal is resolved into a singlet (S) and doublet (D). The singlet signal represents the 1.11% natural abundance ^{13}C while the doublet signal represents the contribution of [4,5,6-$^{13}C_3$] and [5,6-$^{13}C_2$]hexose isotopomers, shown schematically on the left. The resonance marked "x" is an unassigned ^{13}C NMR signal not related to glucose.

3.2. Hepatic Krebs cycle ^{13}C-enrichment and meta0bolic fluxes from PAGN analysis

Urinary PAGN was produced by all subjects in quantities ranging from 150 to 400 μmol. In contrast to a recent study of phenylbutyrate metabolism that documented the urinary production of both PAGN and phenylbutyrylglutamine (Comte et al., 2002), only PAGN was detected in our samples as determined by ^{1}H NMR analysis of both crude and purified urine fractions. The phenylbutyrate dose used in our study was an order of magnitude smaller than that described in the study of Comte et al. and may explain its more efficient conversion to PAGN. The ^{13}C NMR signals of PAGN recovered from both controls and GSD1a patients revealed ^{13}C–^{13}C spin coupled multiplets in the five carbons of the glutamine moiety. Multiplets from carbons 2, 3 and 4 of the glutamine moiety were selected for quantification of ^{13}C-isotopomers because of their higher signal-to-noise ratios under the NMR acquisition conditions (short repetition time and proton decoupling with nuclear Overhauser effect (nOe)) in comparison to the carbon 1 and 5 carboxyl resonances. The carboxyl signals were much weaker due to the absence of nOe and also because of extensive saturation resulting from their long spin-lattice relaxation times. Moreover, the isotopomer information from the ^{13}C-multiplet signals of carbons 1 and 5 is redundant under our study conditions (i.e. the [4,5-$^{13}C_2$]glutamine isotopomer that forms the doublet signal of carbon 5 is also represented by the doublet signal of carbon 4 while isotopomers that contribute to the carbon 1 doublet; [1,2-$^{13}C_2$]glutamine and [1,2,3-$^{13}C_3$]glutamine, are also represented in the carbon 2 multiplet). Fig. 4 shows the ^{13}C resonances of carbons 2, 3 and 4 from a healthy subject and GSD1a patient 1, who had no detectable ^{13}C-enrichment of glucose or glucuronide. The presence of significant levels of glutamine carbon 4 enrichment (see Table 2), invalidates the estimation of anaplerotic, pyruvate recycling and gluconeogenic fluxes directly from the carbon 2 multiplet ratios (Jones et al., 1997). Nevertheless, inspection of the multiplets and ^{13}C-isotopomer ratios provides some qualitative information on the hepatic flux profiles. Carbons 4 and 5 of PAGN originate from carbons 2 and 1 of acetyl-CoA, hence the presence of [4,5-$^{13}C_2$]glutamine indicates the production of [1,2-$^{13}C_2$]acetyl-CoA from [U-^{13}C]pyruvate via pyruvate dehydrogenase. For all subjects, the D23 doublet signal of carbon 2 was substantially higher than the quartet (Q) contribution, reflecting a large excess of [2,3-$^{13}C_2$]glutamine relative to [1,2,3-$^{13}C_3$]glutamine and indicative of extensive pyruvate recycling (Jones et al., 1997,

Table 1
Urinary glucuronide and plasma glucose carbon 6 ^{13}C NMR signal ratios (C6D, C6S), excess glucuronide and glucose carbon 6 enrichments, and the fraction of plasma glucose derived from hepatic G6P derived from glucose and glucuronide excess enrichments.

	Glucuronide C6D/(C6D+C6S)	Glucose C6D/(C6D+C6S)	Glucuronide C6 excess enrichment	Glucose C6 excess enrichment	Percent of glucose derived from G6P
Controls					
1	0.64	0.42	1.97	0.80	41
2	0.49	0.32	1.07	0.52	49
3	0.65	0.25	2.06	0.37	18
4	0.63	0.43	1.89	0.84	44
5	0.60	0.26	1.67	0.39	23
Mean ± S.D.	0.60 ± 0.06	0.34 ± 0.09	1.73 ± 0.40	0.58 ± 0.22	35 ± 14
GSD1a					
1	0.00	0.00	0.00	0.00	0
2	0.17	0.00	0.22	0.00	0
3	0.07	0.00	0.08	0.00	0
4	0.21	0.00	0.30	0.00	0
5	0.34	0.00	0.57	0.00	0
Mean ± S.D.	0.16 ± 0.13	0.00 ± 0.00	0.23 ± 0.22	0.00 ± 0.00	0 ± 0

Please cite this article as: Jones, J.G., et al., Hepatic anaplerotic outflow fluxes are redirected from gluconeogenesis to lactate synthesis in patients with Type 1a glycogen storage disease. Metab. Eng. (2009), doi:10.1016/j.ymben.2009.01.003

1998, 2001). Metabolic flux analysis by tcaCALC is summarized in Fig. 5 and the flux outputs reflect the qualitative metabolic profile gleaned from inspection of the PAGN ^{13}C-multiplets. In control subjects, about one-third of acetyl-CoA utilized by the Krebs cycle was derived from pyruvate oxidation via pyruvate dehydrogenase (PDH). The fractional contribution of PDH flux to the acetyl-CoA pool was significantly higher in the GSD1a subjects, accounting for over one-half of acetyl-CoA generation. This difference in PDH flux contribution to acetyl-CoA is evident by a greater intensity of the carbon 4 doublet signal relative to that of carbon 3 for GSD1a patients, as illustrated by the spectra in Fig. 4. This reflects a higher abundance of [4,5-$^{13}C_2$]glutamine relative to the other ^{13}C-isotopomers in GSD1a subjects compared to controls (see Table 2). In the metabolic model of the Krebs cycle, [U-^{13}C]pyruvate oxidation to acetyl-CoA is well defined by the enrichment level of [4,5-$^{13}C_2$]glutamine and this isotopomer signal could be measured with high precision in the ^{13}C NMR spectrum. For each subject, this translated into narrow confidence intervals (typically 10–30% of the flux estimate, see Table 3) as estimated by Monte-Carlo simulations.

In healthy subjects, flux through pyruvate carboxylase, PEP-carboxykinase and pyruvate kinase, constituting the pyruvate cycling pathway, was an order of magnitude higher than the oxidative Krebs cycle flux indicating high pyruvate cycling activity (Jones et al., 1997, 1998, 2001). Net anaplerotic outflow was about 1.5 times that of oxidative Krebs flux and amounted to ~10% of the pyruvate cycling activity. In GSD1a subjects, pyruvate cycling fluxes were even higher than those of controls. Despite the blockage of gluconeogenic outflow, net anaplerotic fluxes also tended to be higher in GSD1a patients, amounting to about twice that of oxidative Krebs cycle flux. These results need to be interpreted with caution since the anaplerotic and pyruvate kinase flux estimates of each subject were associated with larger confidence intervals (~50–150% of the flux values, see Table 3) compared with those obtained for pyruvate oxidation flux. There are two reasons for this: first, the ^{13}C-glutamine isotopomers that define anaplerotic and pyruvate cycling fluxes, notably [1,2-$^{13}C_2$]glutamine and [1,2,3-$^{13}C_3$]glutamine, were present in low abundance as seen by their respective D12 and Q signals in the carbon 2 resonance of Fig. 4. Thus, the quantification of these signals was less certain compared to those from other ^{13}C-

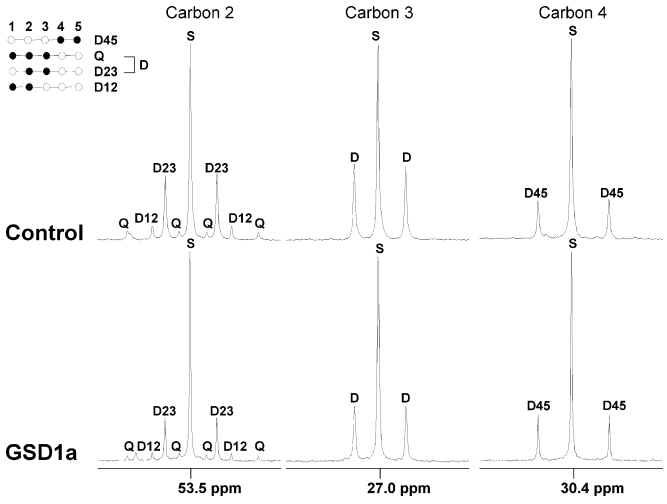

Fig. 4. ^{13}C NMR multiplet signals of phenylacetylglutamine carbons 2, 3 and 4 from a healthy control and from GSD1a patient 1 that had no ^{13}C-enrichment of either glucuronide or glucose. Each multiplet is resolved into isotopomer components as follows: carbon 2; S = natural abundance singlet signal, D12 = doublet reflecting ^{13}C in both positions 1 and 2, D23 = doublet reflecting ^{13}C in both positions 2 and 3, Q = quartet reflecting ^{13}C in positions 1, 2 and 3, Carbon 3; S = natural abundance singlet signal, D = doublet reflecting ^{13}C in both positions 2 and 3 regardless of position 1, carbon 4; S = natural abundance singlet signal, D45 = doublet reflecting ^{13}C in both positions 4 and 5. Hepatic glutamine ^{13}C-isotopomers represented by the ^{13}C NMR signals are shown schematically on the top left-hand side.

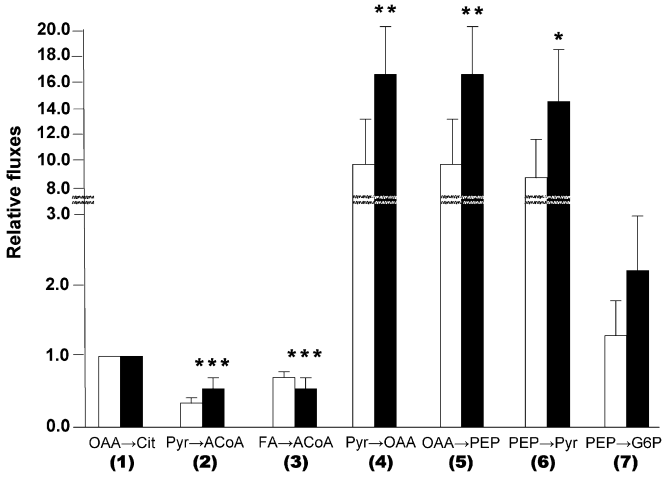

Fig. 5. Relative flux estimates for selected metabolite transformations for healthy subjects (white) and GSD1a patients (black). Data represent the mean values for each group. The error bar on each column represents the standard deviation of the mean. $^{***}p<0.01$ relative to healthy controls; $^{**}p<0.025$ relative to healthy controls, $^{*}p<0.05$ relative to healthy controls.

Table 2
Hepatic glutamine ^{13}C-isotopomer abundances and excess ^{13}C-enrichments derived from the analysis of the carbon 2, 3 and 4 ^{13}C NMR signals of urinary phenylacetylglutamine.

	Healthy controls						GSD1a patients					
	1	2	3	4	5	Mean±S.D.	1	2	3	4	5	Mean±S.D.
^{13}C-isotopomer abundances (%)												
[1,2-$^{13}C_2$]PAGN	0.06	0.07	0.08	0.15	0.17	0.10±0.05	0.04	0.07	0.04	0.09	0.07	0.06±0.02
[2,3-$^{13}C_2$]PAGN	0.57	0.56	0.72	0.81	0.86	0.70±0.13	0.35	0.53	0.48	0.87	0.43	0.53±0.20
[1,2,3-$^{13}C_3$]PAGN	0.12	0.14	0.16	0.21	0.20	0.17±0.04	0.09	0.12	0.12	0.27	0.12	0.14±0.07
[4,5-$^{13}C_2$]PAGN	0.22	0.23	0.09	0.41	0.65	0.32±0.21	0.31	0.45	0.18	0.70	0.29	0.39±0.20
^{13}C-Excess enrichment (%)												
Carbon 2	0.74	0.78	0.95	1.15	1.22	0.97±0.21	0.49	0.75	0.66	1.22	0.66	0.76±0.27
Carbon 3	0.65	0.68	0.76	0.84	0.90	0.77±0.11	0.41	0.61	0.64	0.90	0.52	0.62±0.18
Carbon 4	0.22	0.23	0.09	0.41	0.65	0.32±0.21	0.31	0.45	0.18	0.70	0.29	0.39±0.20

Please cite this article as: Jones, J.G., et al., Hepatic anaplerotic outflow fluxes are redirected from gluconeogenesis to lactate synthesis in patients with Type 1a glycogen storage disease. Metab. Eng. (2009), doi:10.1016/j.ymben.2009.01.003

Table 3
Estimates of pyruvate dehydrogenase (PDH), pyruvate carboxylase (YPC) and pyruvate kinase (PK) fluxes, relative to a citrate synthase flux of 1.0 obtained by tcaCALC analysis of the PAGN ^{13}C NMR spectra.

Flux estimates	Healthy controls				
	Control 1	Control 2	Control 3	Control 4	Control 5
PDH (±S.D.) [5–95% C.I.]	0.28 (0.01) [0.27–0.29]	0.28 (0.02) [0.25–0.30]	0.29 (0.02) [0.25–0.34]	0.10 (0.01) [0.09–0.11]	0.30 (0.09) [0.14–0.45]
YPC (±S.D.) [5–95% C.I.]	13.48 (0.84) [12.48–15.11]	12.84 (4.28) [10.11–24.20]	7.06 (1.03) [5.92–9.03]	9.89 (0.72) [8.83–11.19]	5.89 (4.42) [2.74–14.33]
PK (±S.D.) [5–95% C.I.]	11.80 (0.58) [11.12–12.87]	10.83 (2.79) [8.81–18.28]	6.10 (0.88) [5.10–8.17]	8.89 (0.62) [7.99–9.95]	5.15 (2.94) [1.48–10.60]
	GSD1a Patients				
	Patient 1	Patient 2	Patient 3	Patient 4	Patient 5
PDH (±S.D.) [5–95% C.I.]	0.66 (0.03) [0.62–0.71]	0.63 (0.05) [0.55–0.72]	0.29 (0.03) [0.24–0.32]	0.63 (0.05) [0.56–0.73]	0.53 (0.06) [0.43–0.64]
YPC (±S.D.) [5–95% C.I.]	14.21 (1.57) [12.40–17.17]	21.92 (N.D.) [14.99–49.96]	12.87 (N.D.) [8.04–28.38]	18.04 (3.80) [14.27–26.10]	15.88 (N.D.) [11.41–28.95]
PK (±S.D.) [5–95% C.I.]	12.76 (1.24) [11.18–15.34]	19.87 (N.D.) [13.30–42.25]	9.55 (9.23) [7.06–19.51]	15.35 (2.84) [12.53–21.33]	14.36 (N.D.) [10.45–26.07]

Also shown are the associated uncertainties obtained by Monte-Carlo simulation. Uncertainties are reported as standard deviation (S.D.) and 5–95% confidence intervals (C.I.). In some cases, the Monte-Carlo simulation did not return standard deviation values, and these are noted as not determined (N.D.).

isotopomers. Moreover, a sensitivity analysis performed with tcaSIM[2] to determine the unit change in anaplerotic and pyruvate recycling fluxes in response to changing the ^{13}C NMR multiplet ratios revealed that these relative flux estimates are quite sensitive to small errors in the D12 and Q multiplet contributions (data not shown).

3.3. Enrichment of plasma and urinary lactate from [U-^{13}C]glycerol

Plasma lactate was enriched with ^{13}C in both healthy and GSD1a subjects. Significant levels of urinary lactate were detected by ^{1}H and ^{13}C NMR in three of the five GSD1a patients while none was detected in healthy subjects. For the three GSD1a patients that had urinary lactate, the carbon 2 and 3 ^{13}C-signals had similar ^{13}C NMR multiplet structures to those of plasma lactate indicating that urinary lactate was also enriched from [U-^{13}C]glycerol. In healthy subjects, plasma lactate levels relative to glucose were 0.30±0.06, as assessed by the natural abundance ^{13}C-lactate/^{13}C-glucose signal ratios. In GSD1a patients, the plasma lactate to glucose ratio was 1.63±1.33 reflecting a much higher availability of lactate relative to glucose as an oxidizable substrate for peripheral tissues. In healthy subjects, ^{13}C-enrichment levels of plasma lactate carbon 3 were estimated to be 0.6±0.3%. These values correspond to the carbon 6 enrichment levels of plasma glucose[3] and are consistent with Cori cycle activity where plasma lactate is derived from peripheral tissue glycolysis of endogenous glucose. In GSD1a patients, plasma and urinary lactate were also enriched with ^{13}C. Plasma lactate carbon 3 enrichment levels were 0.4±0.2%, slightly lower than that of control subjects. However, given the high plasma lactate concentrations and the additional lactate recovered in urine in GSD1a patients, this level of ^{13}C-enrichment represents a much larger mass conversion of [U-^{13}C]glycerol to ^{13}C-lactate compared to that of healthy control subjects. Since plasma glucose was not enriched with ^{13}C in the GSD1a patients, the ^{13}C-lactate enrichment could not have been derived from plasma glucose via the Cori cycle but instead must have been directly derived from the liver. The plasma lactate isotopomer distribution, as shown in Fig. 6, revealed significant amounts of [1,2-$^{13}C_2$] and [2,3-$^{13}C_2$]lactate isotopomers, which are derived from passage of the [U-^{13}C]glycerol moiety through the hepatic Krebs cycle and pyruvate recycling pathways. This indicates that a substantial portion of the ^{13}C-enriched lactate was derived via the anaplerotic fluxes of the Krebs cycle, rather than by direct glycolysis of [U-^{13}C]glycerol (which would only generate the [1,2,3-$^{13}C_3$]lactate isotopomer).

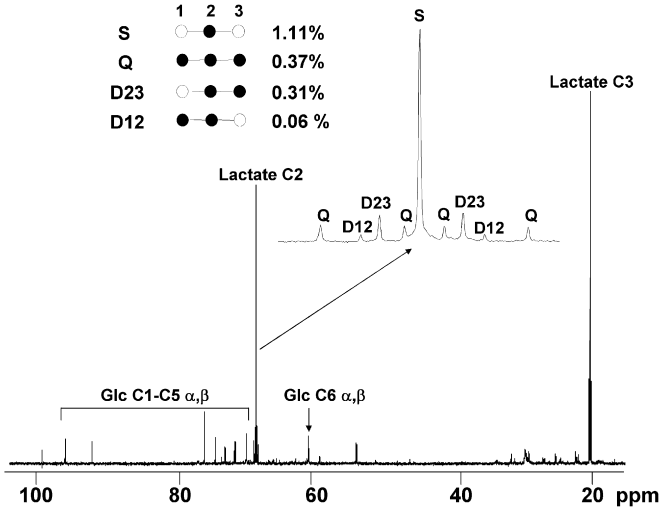

Fig. 6. ^{13}C NMR signals of plasma glucose and lactate from a GSD1a patient. The lactate carbon 2 signal and its ^{13}C–^{13}C spin–spin coupled multiplets are shown in expanded form. The carbon 2 multiplet is resolved into isotopomer components as follows: carbon 2; S = natural abundance singlet signal, D12 = doublet reflecting ^{13}C in both positions 1 and 2, D23 = doublet reflecting ^{13}C in both positions 2 and 3, Q = quartet reflecting ^{13}C in positions 1, 2 and 3 reflecting ^{13}C in both positions 4 and 5. The identity and abundance of lactate ^{13}C-isotopomers represented by the ^{13}C NMR signals of carbon 2 are shown schematically to the left.

4. Discussion

In this study, the complete block of carbon flow from hepatic intermediary metabolites to glucose in GSD1a patients was confirmed using a gluconeogenic tracer. In previous metabolic tracer studies of GSD1 children, [U-^{13}C]glucose was given by nasogastric infusion and plasma glucose was analyzed for ^{13}C-isotopomers (Kalderon et al., 1988, 1989). Under normal conditions, metabolism of infused [U-^{13}C]glucose generates a population of partially labeled ^{13}C-glucose molecules through the recycling of ^{13}C-tracer via glycolysis, hepatic gluconeogenesis and glucose production (Tayek and Katz, 1996). In GSD1a patients,

[2] tcaSIM is also available from http://www.utsouthwestern.edu/utsw/home/research/AIRC.

[3] Glucose enriched with ^{13}C in carbon 6 (and/or carbon 1) will generate lactate enriched in carbon 3.

Please cite this article as: Jones, J.G., et al., Hepatic anaplerotic outflow fluxes are redirected from gluconeogenesis to lactate synthesis in patients with Type 1a glycogen storage disease. Metab. Eng. (2009), doi:10.1016/j.ymben.2009.01.003

these isotopomers were not detected, consistent with the absence of hepatic glucose production from G6P. In these studies, plasma lactate was enriched with ^{13}C and in addition to [U-^{13}C]lactate derived by simple glycolysis, lactate ^{13}C-isotopomers containing one or two ^{13}C atoms were also detected. These latter isotopomers are generated during passage of the [U-^{13}C]pyruvate moiety through the anaplerotic pathways of the hepatic Krebs cycle. While these studies provide evidence for blocked hepatic glucose production and the involvement of the hepatic Krebs cycle in the synthesis of ^{13}C-lactate from [U-^{13}C]glucose, the ^{13}C-isotopomer information from plasma glucose and lactate is not sufficient for describing specific hepatic Krebs cycle fluxes.

In current models of human hepatic intermediary metabolism, gluconeogenesis is assumed to be the main pathway for anaplerotic carbon outflow from the hepatic Krebs cycle (Magnusson et al., 1991; Esenmo et al., 1992; Landau et al., 1993; Large et al., 1997; Diraison et al., 1998; Jones et al., 2001; Burgess et al., 2003). This assumption is based on the fact that under most conditions, gluconeogenic flux is much higher than other potential net outflow fluxes from the hepatic Krebs cycle, such as amino acid or citrate synthesis. Although several independent studies have focused on quantifying human gluconeogenic and oxidative hepatic Krebs cycle fluxes from the labeling distribution of hepatic glutamine from a gluconeogenic tracer, estimates of human gluconeogenic outflow relative to oxidative Krebs cycle activity (i.e. flux through citrate synthase) remain highly uncertain, possibly because of systematic methodological biases in the determination of hepatic Krebs cycle fluxes with different tracers and analytical techniques. Based on the incorporation of [3-^{14}C]lactate tracer into carbons 1–5 of PAGN, Magnusson et al. (1991) estimated that gluconeogenic fluxes were 2–3 times that of citrate synthase flux. These relative flux ratios were similar between 60-h fasted subjects and overnight-fasted subjects given a glucose load. In a stable-isotope study using [3-^{13}C]lactate and analysis of positional ^{13}C-enrichment in PAGN by gas chromatography-mass spectrometry, gluconeogenic fluxes were estimated to be ~0.5 times those of citrate synthase flux in overnight-fasted healthy subjects (Diraison et al., 1998). Jones et al. (1998, 2001) reported gluconeogenic flux values that were approximately equal to citrate synthase flux in overnight-fasted subjects and ~1.4 times citrate synthase flux in 24-h fasted subjects using [U-^{13}C]propionate as a gluconeogenic tracer and ^{13}C NMR analysis of PAGN ().

Estimates of pyruvate recycling fluxes based on phenylacetylglutamine labeling from [3-^{13}C] or [3-^{14}C]lactate tracers, are typically smaller than those derived from this study or in previous studies using [U-^{13}C]propionate (Jones et al., 1998, 2001). Pyruvate recycling fluxes of 4 times citrate synthase flux were reported in 60-h fasted healthy subjects infused with [3-^{14}C]lactate (Magnusson et al., 1991) while for overnight-fasted subjects infused with [3-^{13}C]lactate, pyruvate recycling flux was estimated to be ~2 times citrate synthase flux (Diraison et al., 1998). In common with the ^{13}C-isotopomer methodology presented here, estimates of pyruvate cycling fluxes from [3-^{13}C]- or [3-^{14}C]lactate are also subject to high uncertainty because they require quantification of ^{13}C-enrichment or ^{14}C-specific activity in carbon 5 relative to carbons 2 and 3 of phenylacetylglutamine. Under most conditions, carbon 5 labeling from these tracers is very low relative to the other positions and small errors in the measurement of carbon 5 labeling propagate large errors in pyruvate recycling flux estimates.

The metabolic model assumes metabolic and isotopic steady-state conditions. To the extent that the ^{13}C-enrichment levels of triose phosphate and pyruvate were varying over time as the ^{13}C-glycerol tracer was taken up by the liver and then consumed, a constant precursor ^{13}C-enrichment level was not maintained in our study. For both control and GSD1a subjects, the sampling period represented the peak ^{13}C-enrichment levels of glucuronide and phenylacetylglutamine; i.e. ^{13}C-enrichment levels for these metabolites were less for urine samples collected before or after this interval (data not shown). Under metabolic steady-state conditions the Krebs cycle flux parameters are relatively insensitive to slow changes in ^{13}C-precursor enrichment (Jones et al., 1998) hence these values are not expected to be significantly influenced by washing-in and out of the ^{13}C-label. We surmise that the 3-hourly cornflour ingestion regime maintained a relatively constant source of absorbed carbohydrate and hepatic metabolic state, but we acknowledge that other settings such as an insulin/glucose clamp protocol could provide more precise metabolic and endocrine control.

Hepatocyte intermediary metabolism is characterized by high activities of anaplerotic enzymes such as pyruvate carboxylase, the capacity to utilize a wide range of anaplerotic substrates, and an abundance of these substrates in the portal vein flow. Our results with GSD1a patients suggest that a restriction in gluconeogenic flux imposed from the top down results in a significant redistribution of carbon fluxes at the level of the hepatic Krebs cycle. These include an increased recruitment of acetyl-CoA from pyruvate relative to fatty acid oxidation and increased pyruvate recycling fluxes. These alterations are accompanied by predictable changes in the ^{13}C-isotopomer distribution of hepatic glutamine. In contrast, a change in the destination of anaplerotic outflow has no effect on the glutamine ^{13}C-isotopomer distribution and is therefore undefined by glutamine ^{13}C-isotopomer analysis. Thus, while relative anaplerotic fluxes in GSD1a patients were similar to those of healthy controls, the principal destination of anaplerotic carbons in GSD1a patients was lactate instead of G6P. As a result, gluconeogenic flux was decoupled from net anaplerotic outflow. In healthy subjects, the extent to which anaplerotic efflux is diverted from gluconeogenesis to lactate production is difficult to resolve by the analysis of lactate ^{13}C-enrichment from ^{13}C-tracers of the hepatic Krebs cycle. This is because plasma lactate can become enriched with ^{13}C via the Cori cycle (i.e. via gluconeogenesis, hepatic glucose production and peripheral tissue glycolysis) as well as by direct anaplerotic outflow from the hepatic Krebs cycle.

The utilization of acetyl-CoA by lipogenesis provides another means for the non-oxidative disposal of carbon from the hepatic Krebs cycle pool. While de novo lipogenesis fluxes are relatively small in comparison to Krebs cycle and gluconeogenic fluxes in healthy subjects, in the few studies performed on GSD1a subjects, de novo lipogenesis rates of up to 40 times that of healthy controls were reported (Bandsma et al., 2002a, 2002b). If the removal of acetyl-CoA for lipogenesis is compensated by an increase in acetyl-CoA production from pyruvate, oxidative Krebs cycle fluxes will not be changed. Therefore, in the absence of an independent measurement of lipogenesis or pyruvate oxidation, it is not possible to quantify the lipogenic recruitment of acetyl-CoA from the analysis of glutamine ^{13}C-isotopomers. Finally, there is the possibility that while relative anaplerotic fluxes were similar between healthy and GDS1a patients, absolute anaplerotic fluxes might differ if there was a systematic difference in absolute hepatic Krebs cycle fluxes between the two groups. To resolve this would require an independent measure of oxidative hepatic Krebs cycle activity, such as hepatic oxygen consumption or urea production.

In summary, our studies demonstrate that in GSD1a patients, Krebs cycle fluxes are redirected to dispose carbon that would normally be used for glucose synthesis. The redirection of anaplerotic flux from gluconeogenesis to lactate production may be an important part of this adaptation. This mechanism could also play a role in the regulation of gluconeogenesis in healthy

Please cite this article as: Jones, J.G., et al., Hepatic anaplerotic outflow fluxes are redirected from gluconeogenesis to lactate synthesis in patients with Type 1a glycogen storage disease. Metab. Eng. (2009), doi:10.1016/j.ymben.2009.01.003

subjects. The decoupling of gluconeogenic flux from anaplerotic outflow implies that under certain conditions, absolute hepatic Krebs cycle fluxes may need to be evaluated independently of absolute gluconeogenic fluxes.

Acknowledgment

This work was supported by a grant from the Portuguese Foundation of Science and Technology (POCTI/QUI/55603/2004).

References

Bandsma, R.H.J., Smit, G.P.A., Kuipers, F., 2002a. Disturbed lipid metabolism in glycogen storage disease type 1. Eur. J. Pediatr. 161, S65–S69.

Bandsma, R.H.J., Rake, J.P., Visser, G., Neese, R.A., Hellerstein, M.K., van Duyvenvoorde, W., Princen, H.M.G., Stellaard, F., Smit, G.P.A., Kuipers, F., 2002b. Increased lipogenesis and resistance of lipoproteins to oxidative modification in two patients with glycogen storage disease type 1a. J. Pediatr. 140, 256–260.

Beylot, M., Soloviev, M.V., David, F., Landau, B.R., Brunengraber, H., 1995. Tracing hepatic gluconeogenesis relative to citric acid cycle activity in vitro and in vivo. Comparisons in the use of [3-^{13}C]lactate, [2-^{13}C]acetate, and alpha-keto [3-^{13}C]isocaproate. J. Biol. Chem. 270, 1509–1514.

Burgess, S.C., Weis, B., Jones, J.G., Smith, E., Merritt, M.E., Margolis, D., Sherry, A.D., Malloy, C.R., 2003. Noninvasive evaluation of liver metabolism by ^{2}H and ^{13}C NMR isotopomer analysis of human urine. Anal. Biochem. 312, 228–234.

Comte, B., Kasumov, T., Pierce, B.A., Puchowicz, M.A., Scott, M.E., Dahms, W., Kerr, D., Nissim, I., Brunengraber, H., 2002. Identification of phenylbutyrylglutamine, a new metabolite of phenylbutyrate metabolism in humans. J. Mass Spectrom. 37, 581–590.

Diraison, F., Large, V., Brunengraber, H., Beylot, M., 1998. Non-invasive tracing of liver intermediary metabolism in normal subjects and in moderately hyperglycaemic NIDDM subjects. Evidence against increased gluconeogenesis and hepatic fatty acid oxidation in NIDDM. Diabetologia 41, 212–220.

Diraison, F., Large, V., Maugeais, C., Krempf, M., Beylot, M., 1999. Noninvasive tracing of human liver metabolism: comparison of phenylacetate and apoB-100 to sample glutamine. Am. J. Physiol. 277, E529–E536.

Esenmo, E., Chandramouli, V., Schumann, W.C., Kumaran, K., Wahren, J., Landau, B.R., 1992. Use of $^{14}CO_2$ in estimating rates of hepatic gluconeogenesis. Am. J. Physiol. 263, E36–E41.

Fonseca, C.P., Jones, J.G., Carvalho, R.A., Jeffrey, F.M.H., Montezinho, L.P., Geraldes, C., Castro, M., 2005. Tricarboxylic acid cycle inhibition by Li+ in the human neuroblastoma SH-SY5Y cell line: a 13C NMR isotopomer analysis. Neurochem. Int. 47, 385–393.

Hellerstein, M.K., Greenblatt, D.J., Munro, H.N., 1986. Glycoconjugates as noninvasive probes of intrahepatic metabolism-pathways of glucose entry into compartmentalized Hepatic UDP-glucose pools during glycogen accumulation. Proc. Natl. Acad. Sci. USA 83, 7044–7048.

Jin, E.S., Burgess, S.C., Merritt, M.E., Sherry, A.D., Malloy, C.R., 2005. Differing mechanisms of hepatic glucose overproduction in triiodothyronine-treated rats vs. Zucker diabetic fatty rats by NMR analysis of plasma glucose. Am. J. Physiol. 288, E654–E662.

Jones, J.G., Solomon, M.A., Sherry, A.D., Jeffrey, F.M., Malloy, C.R., 1998. ^{13}C NMR measurements of human gluconeogenic fluxes after ingestion of [U-^{13}C]propionate, phenylacetate, and acetaminophen. Am. J. Physiol. 275, E843–E852.

Jones, J.G., Naidoo, R., Sherry, A.D., Jeffrey, F.M.H., Cottam, G.L., Malloy, C.R., 1997. Measurement of gluconeogenesis and pyruvate recycling in the rat liver: a simple analysis of glucose and glutamate isotopomers during metabolism of [1,2,3-$^{13}C_3$]propionate. FEBS Lett. 412, 131–137.

Jones, J.G., Solomon, M.A., Cole, S.M., Sherry, A.D., Malloy, C.R., 2001. An integrated ^{2}H and ^{13}C NMR study of gluconeogenesis and TCA cycle flux in humans. Am. J. Physiol. 281, E848–E851.

Kalderon, B., Lapidot, A., Korman, S.H., Gutman, A., 1988. Glucose recycling and production in children with Glycogen Storage Disease Type-I, studied by gas-chromatography mass-spectrometry and [U-^{13}C]glucose. Biomed. Environ. Mass Spectrom. 16, 305–308.

Kalderon, B., Korman, S.H., Gutman, A., Lapidot, A., 1989. Glucose recycling and production in Glycogenosis Type-I and Type-Iii-stable isotope technique study. Am. J. Physiol. 257, E346–E353.

Katz, J., Wals, P., Lee, W.N., 1993. Isotopomer studies of gluconeogenesis and the Krebs cycle with ^{13}C-labeled lactate. J. Biol. Chem. 268, 25509–25521.

Kien, C.L., Horswill, C.A., Zipf, W.B., McCoy, K.S., Odorisio, T., 1995. Elevated hepatic glucose production in children with Cystic Fibrosis. Pediatr. Res. 37, 600–605.

Landau, B.R., Schumann, W.C., Chandramouli, V., Magnusson, I., Kumaran, K., Wahren, J., 1993. ^{14}C-labeled propionate metabolism in vivo and estimates of hepatic gluconeogenesis relative to Krebs cycle flux. Am. J. Physiol. 265, E636–E647.

Landau, B.R., Wahren, J., Previs, S.F., Ekberg, K., Chandramouli, V., Brunengraber, H., 1996. Glycerol production and utilization in humans: sites and quantitation. Am. J. Physiol. 271, E1110–E1117.

Large, V., Beylot, M., 1999. Modifications of citric acid cycle activity and gluconeogenesis in streptozotocin-induced diabetes and effects of metformin. Diabetes 48, 1251–1257.

Large, V., Brunengraber, H., Odeon, M., Beylot, M., 1997. Use of labeling pattern of liver glutamate to calculate rates of citric acid cycle and gluconeogenesis. Am. J. Physiol. 272, E51–E58.

Magnusson, I., Chandramouli, V., Schumann, W.C., Kumaran, K., Wahren, J., Landau, B.R., 1988. Pentose pathway in human liver. Proc. Natl. Acad. Sci. USA 85, 4682–4685.

Magnusson, I., Schumann, W.C., Bartsch, G.E., Chandramouli, V., Kumaran, K., Wahren, J., Landau, B.R., 1991. Noninvasive tracing of Krebs cycle metabolism in liver. J. Biol. Chem. 266, 6975–6984.

Malloy, C.R., Sherry, A.D., Jeffrey, F.M.H., 1990. Analysis of tricarboxylic acid cycle of the heart using ^{13}C isotope isomers. Am. J. Physiol. 259, H987–H995.

Rognstad, R., Katz, J., 1977. Role of pyruvate kinase in the regulation of gluconeogenesis from L-lactate. J. Biol. Chem. 252, 1831–1833.

Roser, W., Beckmann, N., Wiesmann, U., Seelig, J., 1996. Absolute quantification of the hepatic glycogen content in a patient with glycogen storage disease by ^{13}C magnetic resonance spectroscopy. Magn. Reson. Imaging 14, 1217–1220.

She, P.X., Burgess, S.C., Shiota, M., Flakoll, P., Donahue, E.P., Malloy, C.R., Sherry, A.D., Magnuson, M.A., 2003. Mechanisms by which liver-specific PEPCK knockout mice preserve euglycemia during starvation. Diabetes 52, 1649–1654.

Tayek, J.A., Katz, J., 1996. Glucose production, recycling, and gluconeogenesis in normals and diabetics: a mass isotopomer [U-^{13}C]glucose study. Am. J. Physiol. 270, E709–E717.

Yang, D., Beylot, M., Agarwal, K.C., Soloviev, M.V., Brunengraber, H., 1993. Assay of the human liver citric acid cycle probe phenylacetylglutamine and of phenylacetate in plasma by gas chromatography-mass spectrometry. Anal. Biochem. 212, 277–282.

Please cite this article as: Jones, J.G., et al., Hepatic anaplerotic outflow fluxes are redirected from gluconeogenesis to lactate synthesis in patients with Type 1a glycogen storage disease. Metab. Eng. (2009), doi:10.1016/j.ymben.2009.01.003